Am J Cancer Res 2022;12(12):5403-5424
www.ajcr.us /ISSN:2156-6976/ajcr0147159

Original Article

High beta integrin expression is differentially associated with worsened pancreatic ductal adenocarcinoma outcomes

Matthew GK Benesch[1*], Rongrong Wu[1,2*], Gopal Menon[1*], Kazuaki Takabe[1,3,4,5,6]

[1]Department of Surgical Oncology, Roswell Park Comprehensive Cancer Center, Buffalo, New York 14263, USA; [2]Department of Breast Surgery and Oncology, Tokyo Medical University, Tokyo 160-8402, Japan; [3]Department of Gastroenterological Surgery, Yokohama City University Graduate School of Medicine, Yokohama 236-0004, Japan; [4]Division of Digestive and General Surgery, Niigata University Graduate School of Medical and Dental Sciences, Niigata 951-8520, Japan; [5]Department of Breast Surgery, Fukushima Medical University School of Medicine, Fukushima 960-1295, Japan; [6]Department of Surgery, Jacobs School of Medicine and Biomedical Sciences, State University of New York, Buffalo, New York 14263, USA. [*]Equal contributors.

Received October 21, 2022; Accepted November 27, 2022; Epub December 15, 2022; Published December 30, 2022

Abstract: Outcomes in pancreatic ductal adenocarcinoma (PDAC) are known to be worse in tumors with high integrin β1 expression, but targeted monotherapy against this integrin has not been effective. Seven other beta integrins are expressed in mammalian biology and they are known to have overlapping and compensatory signaling in biological systems. However, their roles in PDAC are poorly understood and have not been systematically compared to integrin β1 biology. In this study, we analyzed the clinical outcomes against beta integrin 1-8 (*ITGB1-8*) expression in PDAC samples from two large independent cohorts, The Cancer Genome Atlas (TCGA) and GSE21501. Biological function and tumor microenvironment composition were studied using Gene Set Enrichment Analysis and xCell. Expression of all eight beta integrins is significantly increased in PDACs relative to normal pancreatic tissues (all $P<0.001$). *ITGB1*, *2*, *5*, and *6* have similarly enriched gene patterns related to transforming growth factor (TGF)-β, epithelial mesenchymal transition, inflammation, stemness, and angiogenesis pathways. Homologous recombination defects and neoantigens are increased in high-*ITGB4, 5,* and *6* tumors, with decreased overall survival in high-*ITGB1, 5,* and *6* tumors compared to low expression tumors (hazard ratios 1.5-2.0). High-*ITGB1, 2*, and *5* tumors have increased fibroblast infiltration (all $P<0.01$) while endothelial cells are increased in high-*ITGB2* and *3* tumors (all $P<0.05$). Overall, beta integrin expression does not correlate to immune cell populations in PDACs. Therefore, while all beta integrins are overexpressed in PDACs, they exert differential effects on PDAC biology. *ITGB2*, *5*, and *6* have a similar profile to *ITGB1*, suggesting that future research in PDAC integrin therapy needs to consider the complementary signaling profiles mediated by these integrins.

Keywords: Bioinformatics, novel therapeutics, desmoplasia, signal transduction, pancreatic cancer

Introduction

Pancreatic ductal adenocarcinoma (PDAC) is a cancer type that remains stubbornly difficult to treat, with 5-year survival rates of about 11% notwithstanding continual advances in surgical, chemotherapy, immunotherapy, and radiotherapy techniques [1]. Despite being the tenth most diagnosed cancer, it is currently third in terms of annual cancers deaths, and it is projected to overtake colorectal cancer for second place within the next five years [1, 2]. Some of the characteristics accounting for its aggressive biology include dense desmoplastic tissue with low tumor mutational burden and a pro-survival milieu that effectively establishes a tumor microenvironment favorable to immune evasion and prone to chemotherapy resistance, coupled with a high metastatic propensity [3, 4].

Decoding and targeting the dense stromal tumor microenvironment (TME) of PDACs is likely one of the most effective strategies to improv-

ing patient outcomes. To this end, integrin signaling within PDACs is an increasing field of translational investigation. Integrins represent a complex family of transmembrane cell adhesion receptors that function as αβ heterodimers comprised from 18 α and 8 β subunits to form at least 24 known pairings in mammalian cells [5]. Their various dimeric pairings facilitate complex extracellular signaling events that result in modulated ligand recruitment to coordinate virtually all aspects of tumor progression [5, 6].

Altered integrin expression patterns exist in multiple malignancies, including PDACs [7]. As the most common β subunit, integrin β1 has been the most studied integrin in PDAC tumorigenesis [8]. β1 integrin signaling is a potent mediator of the epithelial-mesenchymal transition (EMT) phenomenon, which is in part responsible for tumor plasticity via activation of cancer stem cell (CSC) and metastatic pathways [9]. Other studies have shown that disruption of β1 integrin expression can sensitize cancer cells to the anti-angiogenetic drug bevacizumab by increasing levels of reactive oxygen species in endothelial cells [10, 11].

Much research emphasis has been placed on understanding the extracellular matrix (ECM) and desmoplastic reactions that are believed to uniquely contribute to PDAC pathogenesis [12]. The ECM in the PDAC TME is comprised of a dense network of collagen, elastin, and fibronectin proteins incorporating fibroblasts that creates a hypoxic environment conducive to accelerated vascularization and cancer stemness properties, both of which are favorable characteristics for drug resistance and early metastasis [13, 14]. Many of these processes are under the master regulation of transforming growth factor-beta (TGF-β) signaling via fibroblast-to-myofibroblast transdifferentiation and cancer-associated fibroblast (CAF) production of ECM proteins [15]. This orchestra requires primarily β1 integrin-mediated activation of focal adhesion kinase (FAK) to dynamically remodel the ECM to facilitate evolving tumorigenesis among pressures of the immune system and therapy modalities [15-17].

Given the significant position integrin-mediated processes hold in the cancer signaling hierarchy, it comes as no surprise that β1 integrin is an attractive therapeutic target. Among the first such therapies was volociximab, a chimeric monoclonal antibody against the α5β1 integrin heterodimer which suppressed tumor growth in preclinical studies [18]. Through it has been trialed in multiple solid tumor types and is well tolerated, clinical efficacy has not been demonstrated [19, 20]. In a multicenter phase II trial, volociximab did not improve the efficacy of gemcitabine in patients with metastatic PDAC [8], (https://ClinicalTrials.gov/show/NCT00401570). Unfortunately, multiple other β1 integrin-based inhibitors have also lacked clinical efficacy in trials to date [8].

The lack of success thus far in targeting integrin signaling is common in many pathways where ligand or receptor functional redundancy abounds [21]. Single agent therapy, such as in the case of volociximab, is more prone to failure especially since the signaling spectrum of integrins can be both complementary and compensatory following inhibition of any one individual integrin. Cellular processes with redundancy can be some of the most complex biological systems to understand, but their very existence underscores their pivotal contributions to the pathways they underpin. Our understanding of unique and overlapping integrin-mediated processes is primitive at best. Compared to β1 integrin, the research body on beta integrins 2-8 is small and typically siloed by individual integrin type.

In order to gain broader insights into functional redundancies across the eight beta integrins in PDAC, we assessed the beta integrin mRNA expression landscape through *in silico* research approaches [22-25]. We hypothesized that there should be beta integrins with similarly enriched gene sets, tumor microenvironment cell populations, and patient survival characteristics to the β1 integrin that should be concurrently targeted to improve treatment efficacy when designing the next generation of integrin-targeting therapies.

Methods

Data acquisition

Clinical and mRNA expression PDAC data was obtained from the TCGA pancreatic adenocarcinoma (TCGA-PAAD) cohort of 177 patients via the Genomics Data Commons Data Portal (https://portal.gdc.cancer.gov), and a valida-

tion cohort of 132 patients, GSE21501, was obtained from the Gene Expression Omnibus (GEO) repository of the United States National Institutes of Health (https://www.ncbi.nlm.nih.gov/geo), as previously described [22, 26, 27]. Gene expression data from 167 samples of normal pancreatic tissue was obtained from the Genotype-Tissue Expression (GTex) Portal (https://gtexportal.org) [28]. Because all data was obtained from deidentified databases that are available in the public domain, ethics approval requirements were waived by the Roswell Park Institutional Review Board.

Gene set enrichment analysis (GSEA)

Functional enrichment analysis of beta integrin 1-8 (*ITGB1-8*) was performed by GESA [29] on the Molecular Signatures Database Hallmark collection (http://www.gsea-msigdb.org) [30]. Gene sets with a false discovery rate (FDR) <0.25 specified enriched signaling [29].

Other scores

The xCell algorithm (https://xcell.ucsf.edu) [31] was used to correlate beta integrin expression to the infiltrating fraction of TME stromal cells (fibroblasts, endothelial cells, and pericytes), and immune cells (CD8+, T helper cell (Th)1 and Th2 cells, T-regulator cells, M1 and M2 macrophages, and dendritic cells) as previously described [32-35]. MCP-counter was used as a validation algorithm for selected populations [36]. The mutational landscape of PDACs (intratumor heterogeneity, homologous recombination defects, fraction genome altered, silent mutation rate, non-silent mutation rate, single-nucleotide neoantigens, and indel mutations), stromal fraction, TGF-β score, and immune scores (leukocyte fraction, lymphocyte infiltration, tumor infiltration lymphocyte fraction, macrophage regulation, and wound healing) were obtained from Thorsson *et al*. [37]. Immune cytolytic activity (CYT) in the TME was calculated as the geometric mean of the expression of perforin (*PRF1*) and granzyme A (*GZMA*) mRNA expression, which measures the anti-cancer ability of cytotoxic T cells [38].

Statistical analyses

Statistical analyses were conducted with R 4.2.1 software (https://www.R-project.org). Graphics were produced with R software and Origin Pro 2022 (OriginLab Corporation, Northampton, MA, USA). mRNA levels for *ITGB1-8* are dichotomized into low and high groups based on the median expression level. All results are plotted as box plots, with the lower and upper bounds representing the maximum and minimum values, and the upper and lower ends of box representing the 25th and 75th percentile values, and the bolded bar within the box representing the median value. The Mann-Whitney U test is used for comparison between the low and high beta integrin expression groups. The R survival software package was used to analyze progression free survival (PFS), disease-free survival (DFS), disease-specific survival (DSS), and overall survival (OS) based on high or low integrin expression via Cox-proportional hazards regression. $P<0.05$ was set for statistical significance.

Results

Beta integrin expression is elevated in PDAC

We examined whether beta integrin expression is elevated in PDAC compared to normal pancreatic tissue. For all eight beta integrins, mRNA expression is significantly higher in the PDAC specimens compared to normal tissue (all $P<0.001$, **Figure 1**).

ITGB1, 2, 5, and 6 share similar patterns of enriched pathways related to TGF-β, EMT, inflammation, stemness, and angiogenesis

We next used gene set enrichment analysis (GSEA) to investigate Hallmark pathways that are affected for each of the integrins in both cohorts. The complete GSEA output is resulted in Supplemental Table 1. The Hallmark gene sets most upregulated include TGF-β Signaling, Epithelial Mesenchymal Transition (EMT), inflammation-related genesets (Inflammatory Response, TNF-α Signaling via NFκB), stemness-related genesets (Notch Signaling, WNT β-Catenin signaling), angiogenesis-related genesets (Angiogenesis, Hypoxia), and cell proliferation (Mitotic Spindle) (**Figure 2**). The gene set upregulation pattern seen in *ITGB1* was largely replicated and validated in *ITGB2*, *ITGB5*, and *ITGB6*, namely in that TGF-β, EMT, inflammation-related, and angiogenesis-related genesets were upregulated. Genesets upregulated in the TCGA set for *ITGB3* and *ITGB7,* which were similar to the *ITGB1* profile, were not vali-

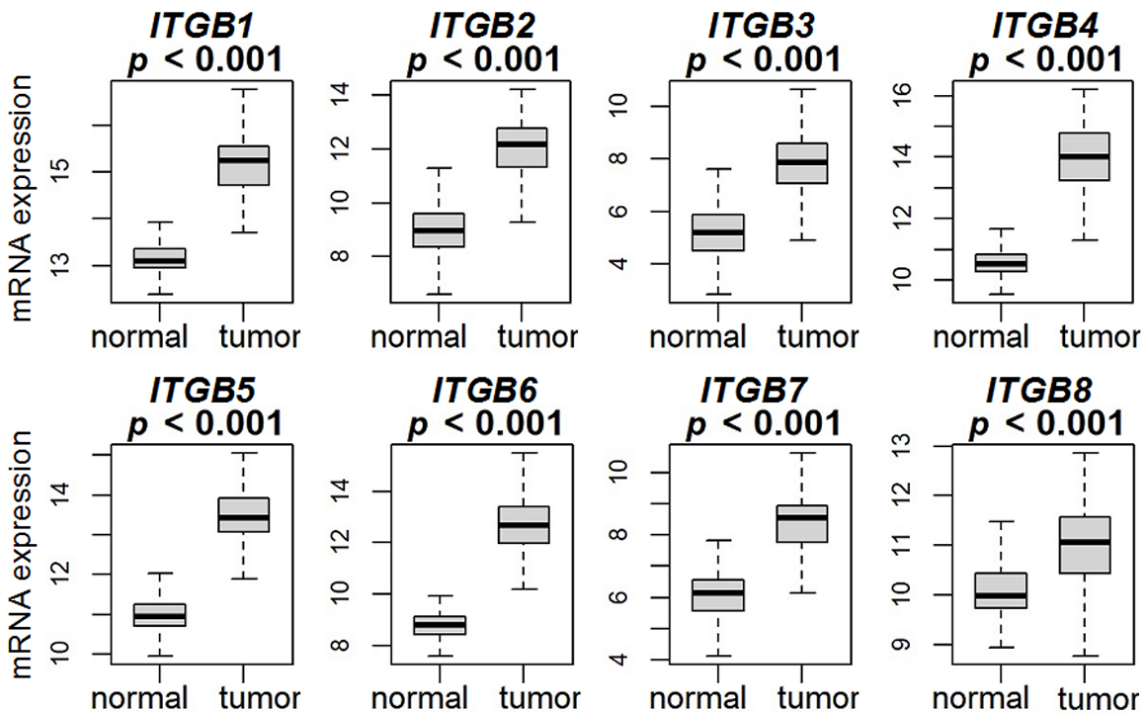

Figure 1. Beta integrin expression is increased in pancreatic cancer specimens compared to normal pancreatic tissues for all beta integrins. mRNA expression from 167 normal pancreas in the GTex database is compared to 177 pancreatic adenocarcinomas in TCGA. Results are plotted as box plots with the bolded center bar representing the median, the lower and upper bounds of the box representing the 25th and 75th percentiles, respectively, and the lower and upper tails representing the minimum and maximum values, respectively.

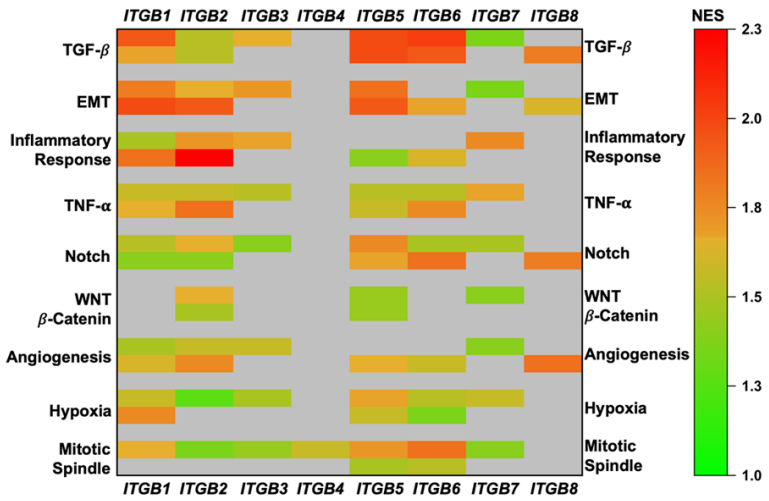

Figure 2. Heatmap of gene set enrichment analysis (GSEA) by beta integrin. The top row in each set represents results from the TCGA cohort and the bottom row from the GSE21501 cohort. A false discovery rate of less than 0.25 was considered statistically significant. NES, Normalized Enrichment Score.

dated in the GSE21501 set, and vise vera for *ITGB8*. The Miotic Spindle gene set was upregulated in TCGA for *ITGB1-7* and validated for *ITGB5-6*. No validated gene sets were upregulated for *ITGB4* (**Figure 2**).

We then analyzed beta integrin expression by tumor stage, grade, and Ki67 expression that all reflect cancer cell proliferation. Consistent with lacking evidence for upregulated cell proliferation pathways by GSEA, there was no robust correlation between stage and expression levels. For *ITGB5*, higher mRNA levels correlated positively to increasing grade in the TCGA cohort (P=0.04), but this was not validated in the GSE21501 cohort (**Figure 3A**). There was also no consistent trend between tumor grade and expression level in the TCGA cohort (**Figure 3B**). Ki67 expression was increased in *ITGB4*-high tumors in the TCGA cohort (P<0.001), but not reproduced in

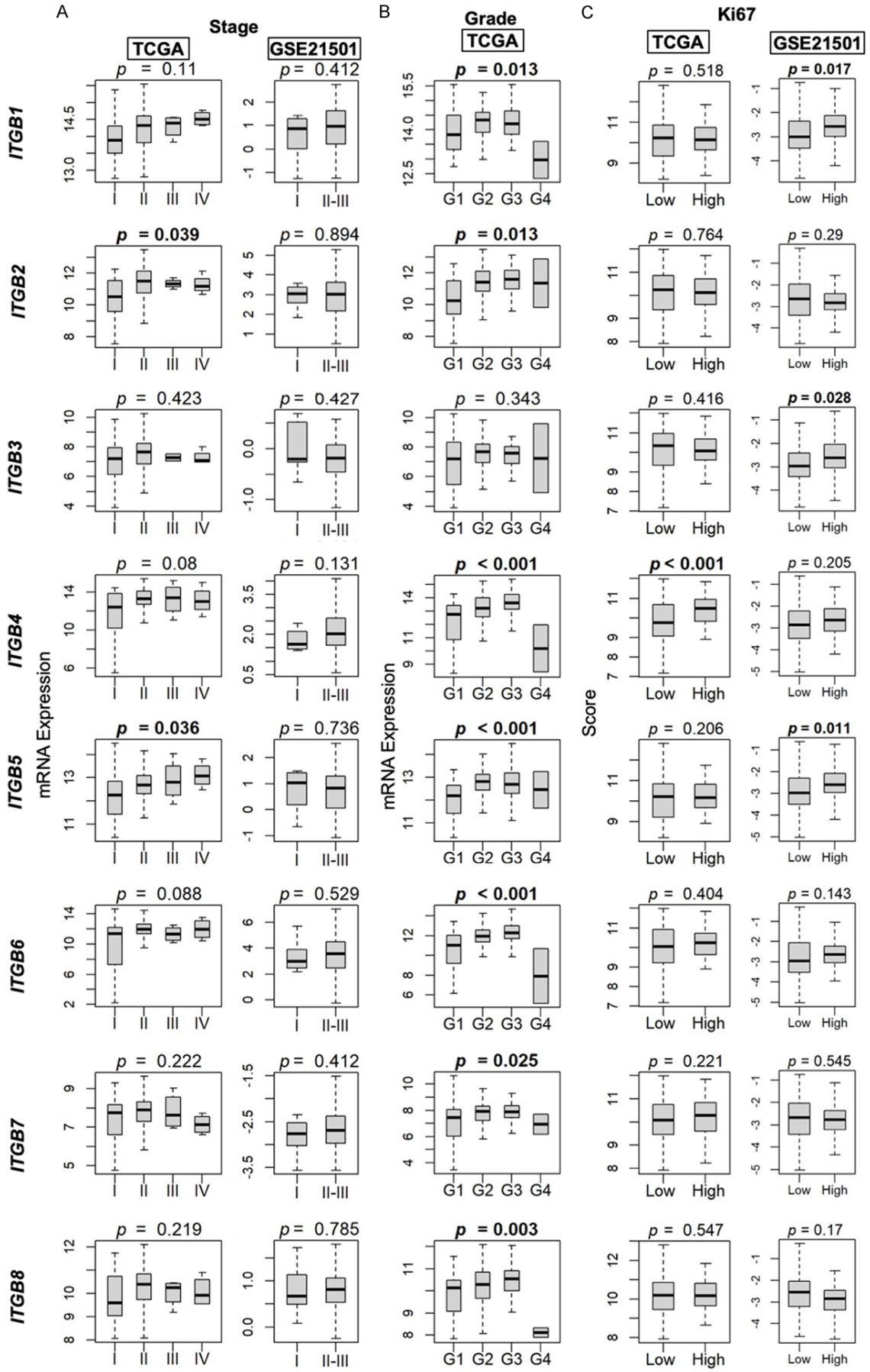
A
Stage
TCGA
GSE21501
B
Grade
TCGA
C
Ki67
TCGA
GSE21501
ITGB1
ITGB2
ITGB3
ITGB4
ITGB5
ITGB6
ITGB7
ITGB8
mRNA Expression
Score
p = 0.11
p = 0.412
p = 0.013
p = 0.518
p = 0.017
p = 0.039
p = 0.894
p = 0.013
p = 0.764
p = 0.29
p = 0.423
p = 0.427
p = 0.343
p = 0.416
p = 0.028
p = 0.08
p = 0.131
p < 0.001
p < 0.001
p = 0.205
p = 0.036
p = 0.736
p < 0.001
p = 0.206
p = 0.011
p = 0.088
p = 0.529
p < 0.001
p = 0.404
p = 0.143
p = 0.222
p = 0.412
p = 0.025
p = 0.221
p = 0.545
p = 0.219
p = 0.785
p = 0.003
p = 0.547
p = 0.17
I II III IV
I II-III
G1 G2 G3 G4
Low High

Figure 3. PDAC stage, grade, and Ki67 scoring by beta integrin. A. Staging according to American Joint Committee on Cancer (AJCC). B. Grading according to AJCC. Grade information not available in the GSE21501 cohort. C. Ki67 scoring dichotomized by median beta integrin expression. Results are plotted as box plots with the bolded center bar representing the median, the lower and upper bounds of the box representing the 25th and 75th percentiles, respectively, and the lower and upper tails representing the minimum and maximum values, respectively.

the GSE21501 cohort, and vice versa for *ITGB3*- and *ITGB5*-high tumors (P=0.03, 0.01 respectively, **Figure 3C**).

Mutation rates are particularly higher in ITGB4, 5, 6-high pancreatic tumors and correlate to worsen survival outcomes

Although pancreatic cancers tend to have low tumor mutational burden, it is a marker of aggressive tumor biology in many cancer types [39]. We next explored whether this might be the case for PDACs by the beta integrin expressions. While intratumor heterogeneity scores were statistically identical between the high and low beta integrin expression groups, homologous recombination defects were significantly increased in *ITGB4, 5*, and *6*-high expression tumors compared to low expression tumors (all P<0.01, **Figure 4A**). Similarly, fraction genome altered, silent mutation rate, nonsilence mutation rate, and SNV neoantigens were all significantly increased in *ITGB4, 5*, and *6*-high expression tumors, except for SNV neoantigens for *ITGB6* (P=0.09, **Figure 4B**). Indel mutations were not different for any of the beta integrins (**Figure 4B**).

Based on these mutation findings, we predicted that high *ITGB4-6* tumors might have worse survival outcomes. Progression-free survival (PFS), disease-free survival (DFS), disease-specific survival (DSS) data was available from the TCGA cohort, and overall survival (OS) from both cohorts (**Figure 5**). Survival data was the most consistently statistically significant for *ITGB5* and *ITGB6*. *ITGB5*-high tumors had worse PFS, DFS, DSS, and OS in the TCGA cohort, but no difference in OS in the GSE21501 cohort. For *ITGB6*, PFS and DSS were worse for *ITGB6* tumors in the TCGA cohort, and OS was decreased in both cohorts. *ITGB1*-high tumors had the same survival pattern as *ITGB5*. *ITGB3*- and *ITGB4*-high tumors had statistically significant worse PFS and DFS. Survival patterns were not particularly robust for *ITGB2, ITGB7,* and *ITGB8,* but the overall trends favored worse survival for the high-expression tumors (**Figure 5**).

Increased fibroblasts content correlates to high-ITGB1, 2, 3, and 5 tumors, and increased endothelial cells are correlated to high-ITGB2 and 3 tumors, but are both decreased in high-ITGB4 tumors

Because PDACs have robust stroma and desmoplasia, we examined the stromal composition of these tumors. The stromal fraction and TGF-β response were increased in beta integrin-high tumors for *ITGB1, 2, 3*, and *5* (all P< 0.05, **Figure 6A**). For *ITGB6*, the stromal fraction was significantly increased (P=0.003), and TGF-β score trended to a significant increase for high tumors (P=0.06). There was no difference between the two groups for *ITGB4, 7,* and *8* (**Figure 6A**). When examined by fibroblast composition using the xCell algorithm, fibroblasts were significantly enriched in both the TCGA and GSE21501 cohorts for high-*ITGB1, 2,* and *5* tumors (all P<0.01), and for high-*ITGB3* tumors in TCGA (P<0.001), but not statistically significant in the GSE21501 cohort (P=0.1, **Figure 6B**). These findings are replicated in the MCP-counter algorithm, except that fibroblasts were significantly enriched in high-*ITGB3* tumors in both cohorts (both P<0.01, **Figure 6C**). Fibroblast levels were decreased in high-*ITGB4* tumors in both cohorts in the xCell algorithm (P<0.01, **Figure 6B**), but not replicated in the MCP-counter algorithm (**Figure 6C**).

As angiogenesis and hypoxia pathways were enriched to some of the integrins (**Figure 2**), we next examined endothelial cell and pericyte level by beta integrin expression. In both cohorts, endothelial cell composition was increased in high-*ITGB2* and *3* tumors in the xCell algorithm (all P<0.05, **Figure 7A**). This was validated in both cohorts for high-*ITGB2* tumors, and for the TCGA cohort for high-*ITGB3* tumors by the MCP-counter algorithm (**Figure 7B**). Endothelial cells were also increased in high-*ITGB1* tumors for the GSE21501 cohort by the xCell algorithm (P<0.001, **Figure 7A**), and in both cohorts by the MCP-counter algorithm (P<0.01, **Figure 7B**). Endothelial cell levels were decreased in high-*ITGB4* tumors in both cohorts and algorithms (all P<0.05, **Figure 7**).

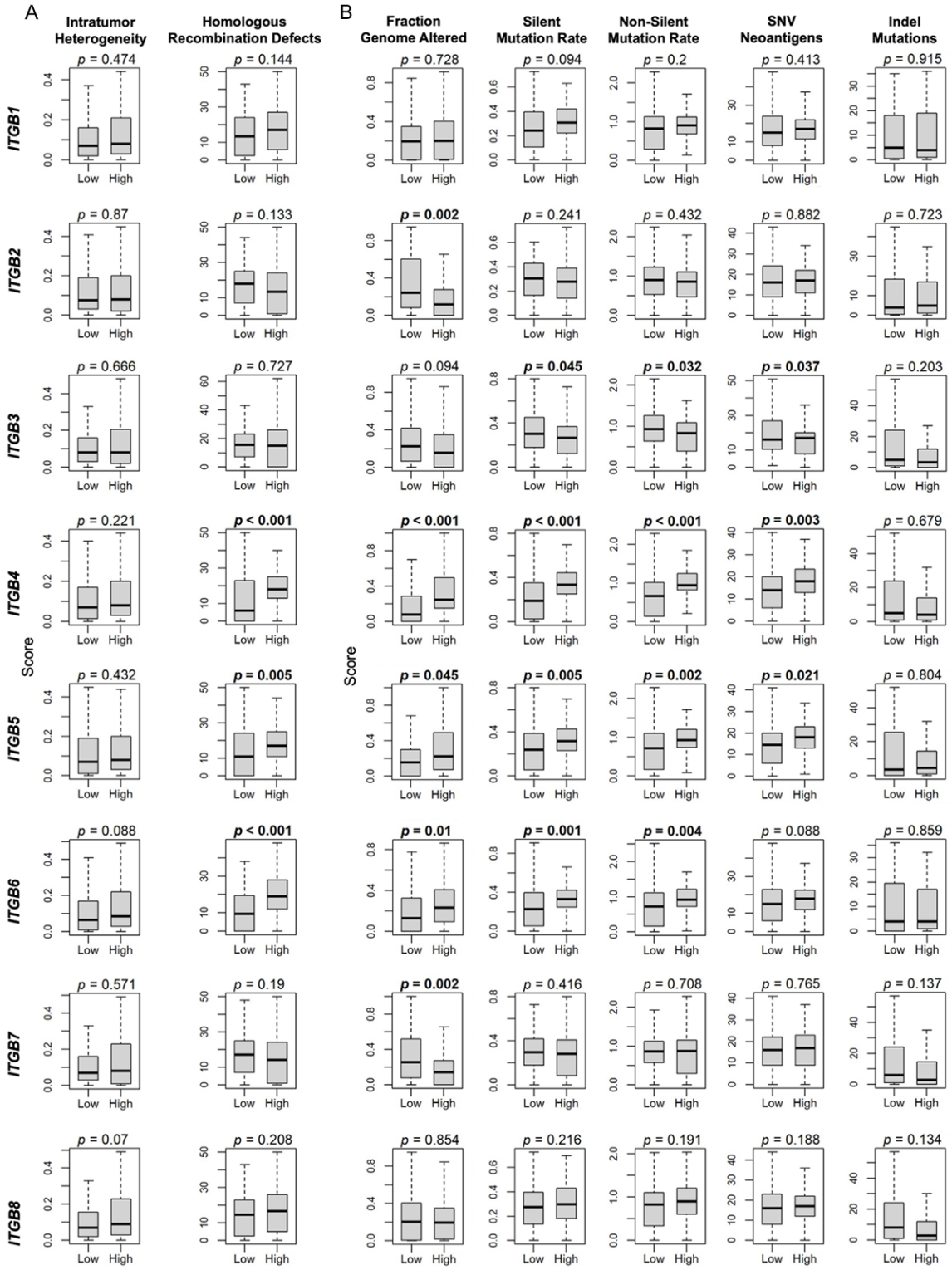

Figure 4. Beta integrin expression correlation with PDAC mutations. A. Box plots of intratumor heterogeneity and homologous recombination defects. B. Box plots of fraction genome altered, silent mutation rate, non-silent mutation rate, single-nucleotide (SNV) variant neoantigens, and indel mutations. The bolded center bar in each box plot represents the median, the lower and upper bounds of the box represent the 25th and 75th percentiles, respectively, and the lower and upper tails represent the minimum and maximum values, respectively. Data is based on the scores by Throsson, *et al.* [37]. Beta-integrin expression is dichotomized into high and low groups by the median, with n=177 for the TCGA cohort and n=132 for the GSE21501 cohort.

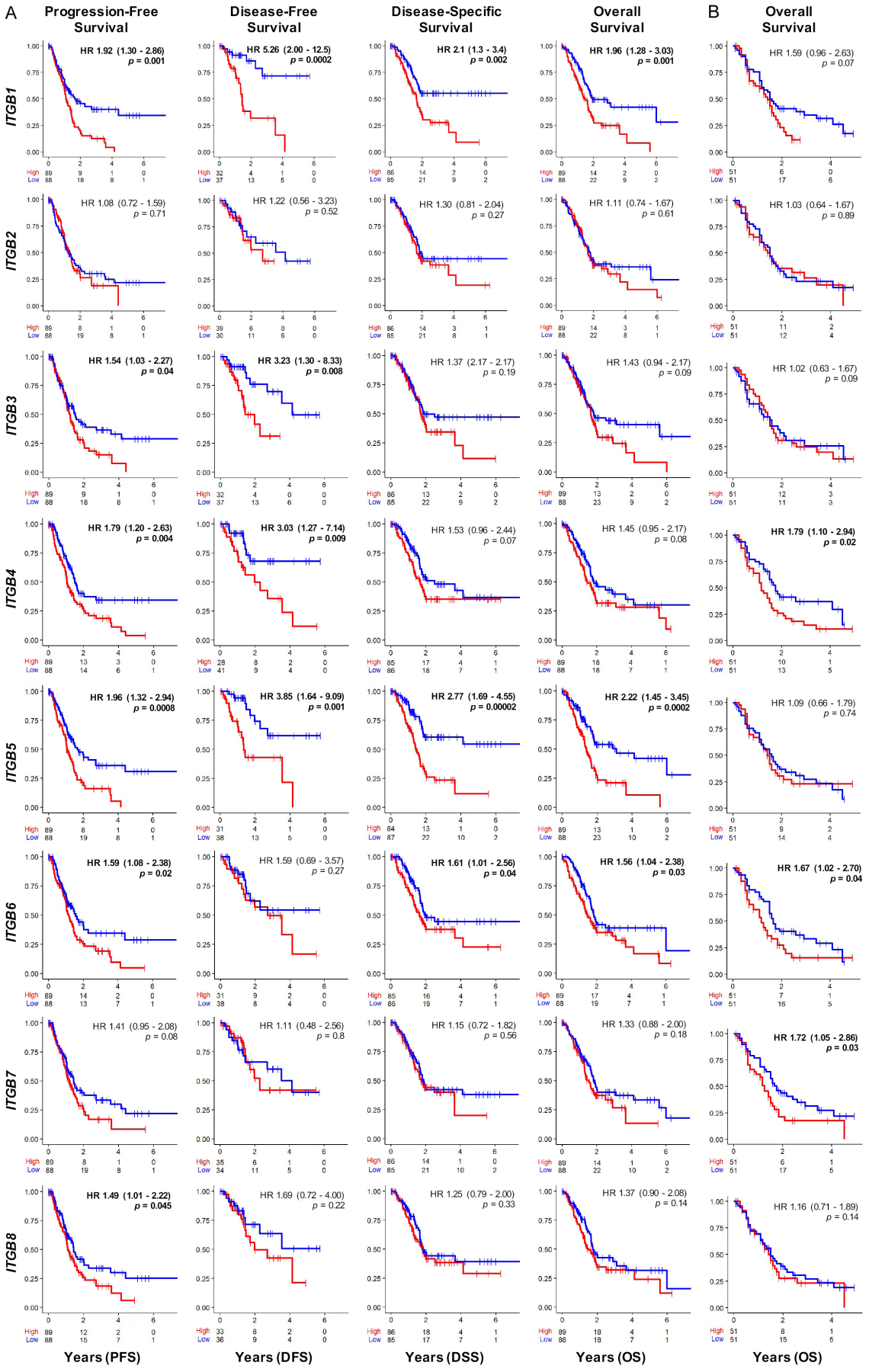
A
Progression-Free Survival
Disease-Free Survival
Disease-Specific Survival
Overall Survival
B
Overall Survival
ITGB1
HR 1.92 (1.30 - 2.86) p = 0.001
HR 5.26 (2.00 - 12.5) p = 0.0002
HR 2.1 (1.3 - 3.4) p = 0.002
HR 1.96 (1.28 - 3.03) p = 0.001
HR 1.59 (0.96 - 2.63) p = 0.07
ITGB2
HR 1.08 (0.72 - 1.59) p = 0.71
HR 1.22 (0.56 - 3.23) p = 0.52
HR 1.30 (0.81 - 2.04) p = 0.27
HR 1.11 (0.74 - 1.67) p = 0.61
HR 1.03 (0.64 - 1.67) p = 0.89
ITGB3
HR 1.54 (1.03 - 2.27) p = 0.04
HR 3.23 (1.30 - 8.33) p = 0.008
HR 1.37 (2.17 - 2.17) p = 0.19
HR 1.43 (0.94 - 2.17) p = 0.09
HR 1.02 (0.63 - 1.67) p = 0.09
ITGB4
HR 1.79 (1.20 - 2.63) p = 0.004
HR 3.03 (1.27 - 7.14) p = 0.009
HR 1.53 (0.96 - 2.44) p = 0.07
HR 1.45 (0.95 - 2.17) p = 0.08
HR 1.79 (1.10 - 2.94) p = 0.02
ITGB5
HR 1.96 (1.32 - 2.94) p = 0.0008
HR 3.85 (1.64 - 9.09) p = 0.001
HR 2.77 (1.69 - 4.55) p = 0.00002
HR 2.22 (1.45 - 3.45) p = 0.0002
HR 1.09 (0.66 - 1.79) p = 0.74
ITGB6
HR 1.59 (1.08 - 2.38) p = 0.02
HR 1.59 (0.69 - 3.57) p = 0.27
HR 1.61 (1.01 - 2.56) p = 0.04
HR 1.56 (1.04 - 2.38) p = 0.03
HR 1.67 (1.02 - 2.70) p = 0.04
ITGB7
HR 1.41 (0.95 - 2.08) p = 0.08
HR 1.11 (0.48 - 2.56) p = 0.8
HR 1.15 (0.72 - 1.82) p = 0.56
HR 1.33 (0.88 - 2.00) p = 0.18
HR 1.72 (1.05 - 2.86) p = 0.03
ITGB8
HR 1.49 (1.01 - 2.22) p = 0.045
HR 1.69 (0.72 - 4.00) p = 0.22
HR 1.25 (0.79 - 2.00) p = 0.33
HR 1.37 (0.90 - 2.08) p = 0.14
HR 1.16 (0.71 - 1.89) p = 0.14
Years (PFS)
Years (DFS)
Years (DSS)
Years (OS)
Years (OS)

Figure 5. Survival plots for high and low beta integrin expression in PDAC. A. Results from the TCGA cohort. B. Results from the GSE21501 cohort. Beta-integrin expression is dichotomized into high and low groups by the median, with n=177 for the TCGA cohort and n=132 for the GSE21501 cohort. HR, Hazard Ratio.

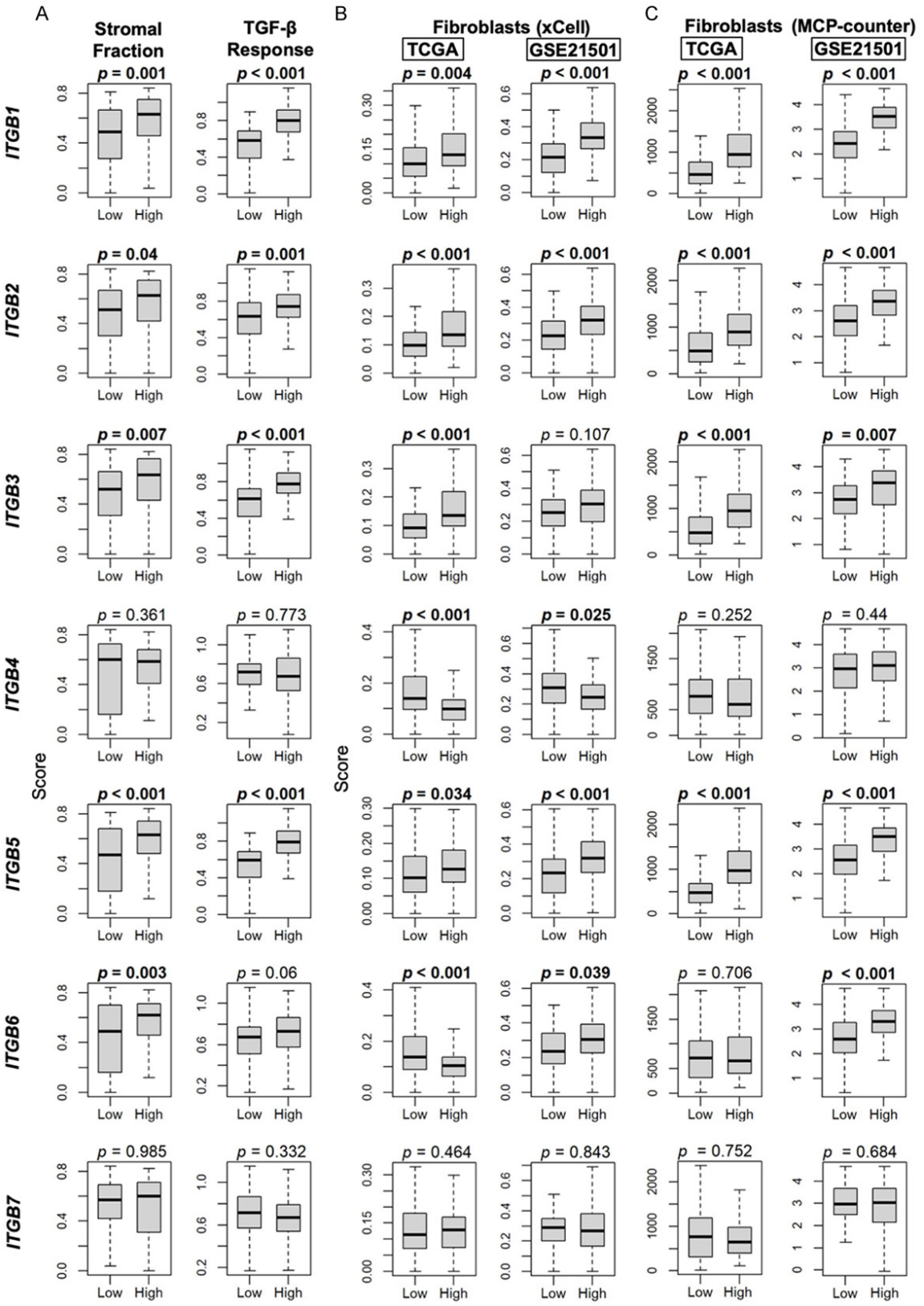

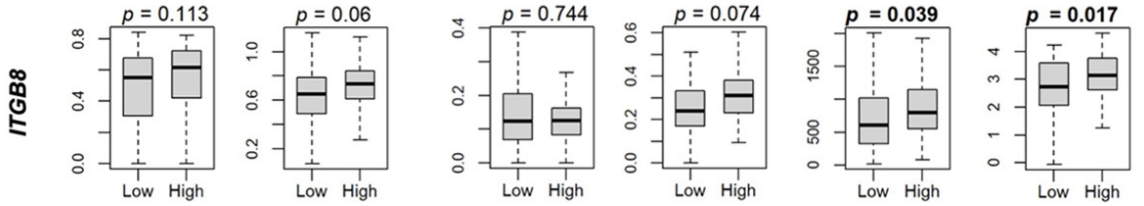

Figure 6. Stromal fraction, TGF-β response, and fibroblast composition correlation with beta integrin expression in PDACs. A. Box plots of calculated scores for stromal fraction and TGF-β response based on Throsson, *et al.* [37]. B. Box plots of fibroblast composition based on the xCell algorithm for the TCGA and GSE21501 cohorts. C. Box plots of fibroblast composition based on the MCP-counter algorithm for the TCGA and GSE21501 cohorts. The bolded center bar in each box plot represents the median, the lower and upper bounds of the box represent the 25th and 75th percentiles, respectively, and the lower and upper tails represent the minimum and maximum values, respectively. Beta-integrin expression is dichotomized into high and low groups by the median, with n=177 for the TCGA cohort and n=132 for the GSE21501 cohort.

Similar trends also occurred in both microvascular endothelial cells (MECs) and lymphatic endothelial cells (LECs) (**Figure 8A**, **8B**). Pericytes were increased in high-*ITGB1, 2, 4*, and *5* tumors in the TCGA cohort (all *P*<0.01), but none of these results were validated in the GSE21501 cohort (**Figure 8C**).

Beta integrin expression does not well correlate with the immune cell population of PDACs

Lastly, we examined the correlation between immune cell populations and beta integrin expression levels. In **Figure 9**, we examined anti-cancerous immune cells between the two cohorts. CD8+ cells were significantly decreased in high-*ITGB4* tumors and T helper 1 (Th1) cells were decreased in high-*ITGB8* tumors (*P*=0.001). M1 macrophages were increased in high-*ITGB1, 2, 5* tumors, and dendritic cells were increased in high-*ITGB2* tumors (all *P*<0.01) (**Figure 9**). We also examined pro-cancerous immune cell populations in the two cohorts, and there were no differences for either regulatory T regulator cells (Tregs) or Th2 cells (**Figure 10**). M2 macrophages were increased in high-*ITGB2* tumors and decreased in high-*ITGB4* tumors (*P*<0.001, **Figure 10**). Examining immune scores by Thorsson *et al.* [37], leukocyte fractions were increased in high-*ITGB2, 3, 7, 8* tumors, and decreased in high-*ITGB4* tumors (all *P*<0.05, **Figure 11**). Lymphocyte infiltration was increased in high-*ITGB2* and *7* tumors, but decreased in high-*ITGB1, 3, 5, 6* tumors (all *P*<0.03, **Figure 11**). Tumor infiltrating lymphocyte (TIL) fraction was increased only in high-*ITGB7* (*P*=0.002) tumors and not significantly changed in other integrins (**Figure 11**). Macrophage regulation and wound healing scores, typically correlate to decreased overall survival [37]. Macrophage regulation scores presented with similar phenotypes to lymphocyte infiltration scores, being increased in high-*ITGB2, 3, 7* tumors and decreased in high-*ITGB4* and *6* tumors (all *P*<0.02, **Figure 11**). Wound healing scores were decreased in high-*ITGB2* tumors and increased in high-*ITGB4* tumors (**Figure 11**). Cytolytic (CYT) scores were only statistically significantly increased in both cohorts for high-*ITGB2* tumors in both xCell and MCP-counter algorithms (*P*<0.001, **Figure 12**). Taken all together, these results illustrate that beta integrin expression did not significantly correlate to the immunotypic profile of PDAC tumors.

Discussion

In this study, we found that all eight beta integrins were significantly upregulated in PDACs compared to normal pancreatic tissues. However, it is also clear that not all beta integrins have similar functions. The characteristics that define prototypical *ITGB1* biology in PDACs were replicated particularly by *ITGB2*, *5,* and *6*. All four integrins had enriched TGF-β pathways, and for high-*ITGB2* and *5* tumors, stromal fractions and tumor fibroblasts were increased to levels mirroring high-*ITGB1* tumors in both cohorts examined. It is well established that tumor desmoplasia is associated with therapy resistance because dense stroma produces relative high extracellular pressure that inhibits systemic drug from penetrating tumor tissue [40].

However, when we look at the effects of high *ITGB1, 2, 5,* and *6* on survival, *ITGB2* was

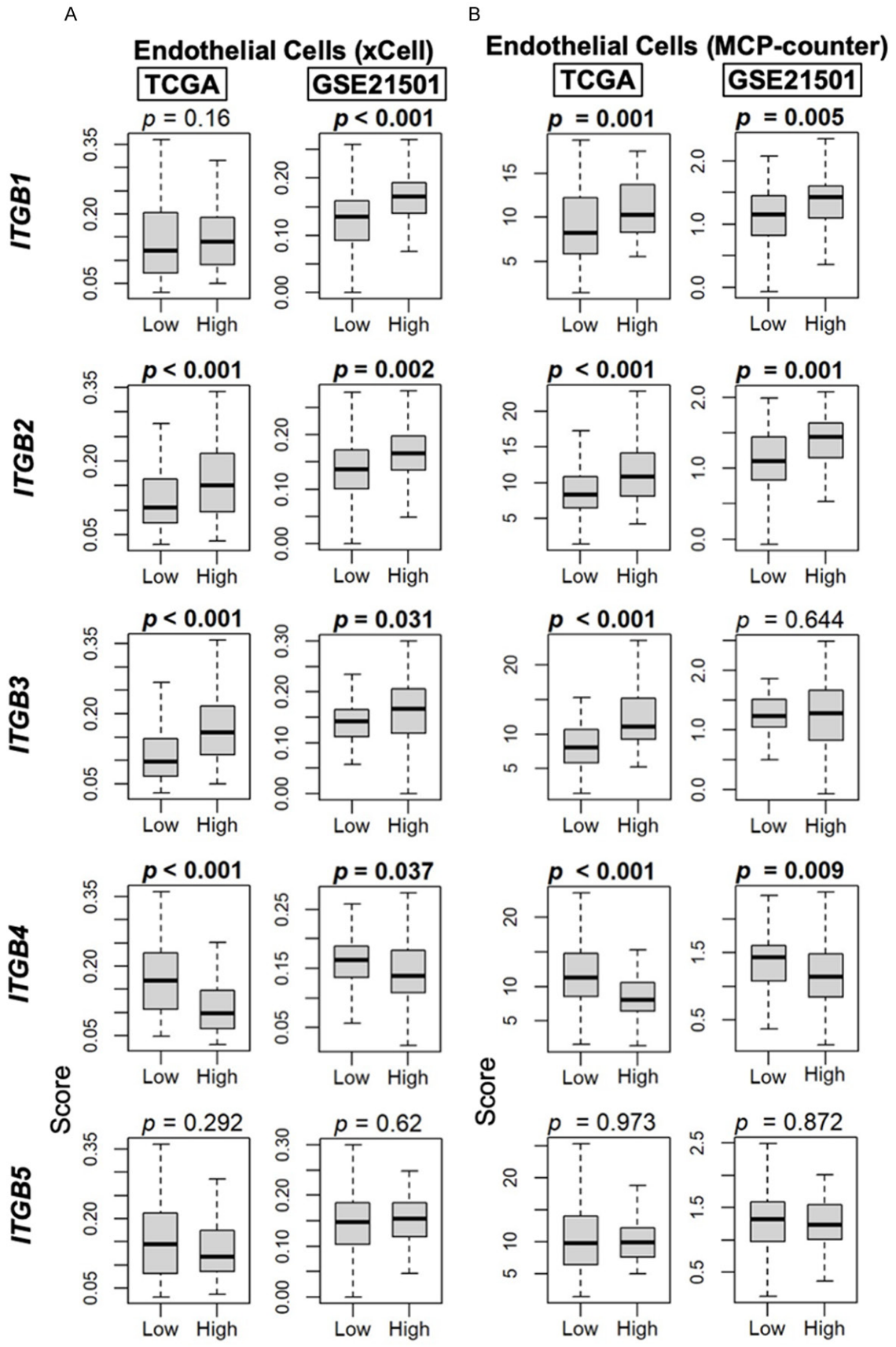
A
B
Endothelial Cells (xCell)
Endothelial Cells (MCP-counter)
TCGA
GSE21501
ITGB1
ITGB2
ITGB3
ITGB4
ITGB5
p = 0.16
p < 0.001
p = 0.001
p = 0.005
p < 0.001
p = 0.002
p < 0.001
p = 0.001
p < 0.001
p = 0.031
p < 0.001
p = 0.644
p < 0.001
p = 0.037
p < 0.001
p = 0.009
p = 0.292
p = 0.62
p = 0.973
p = 0.872
Low
High
Score

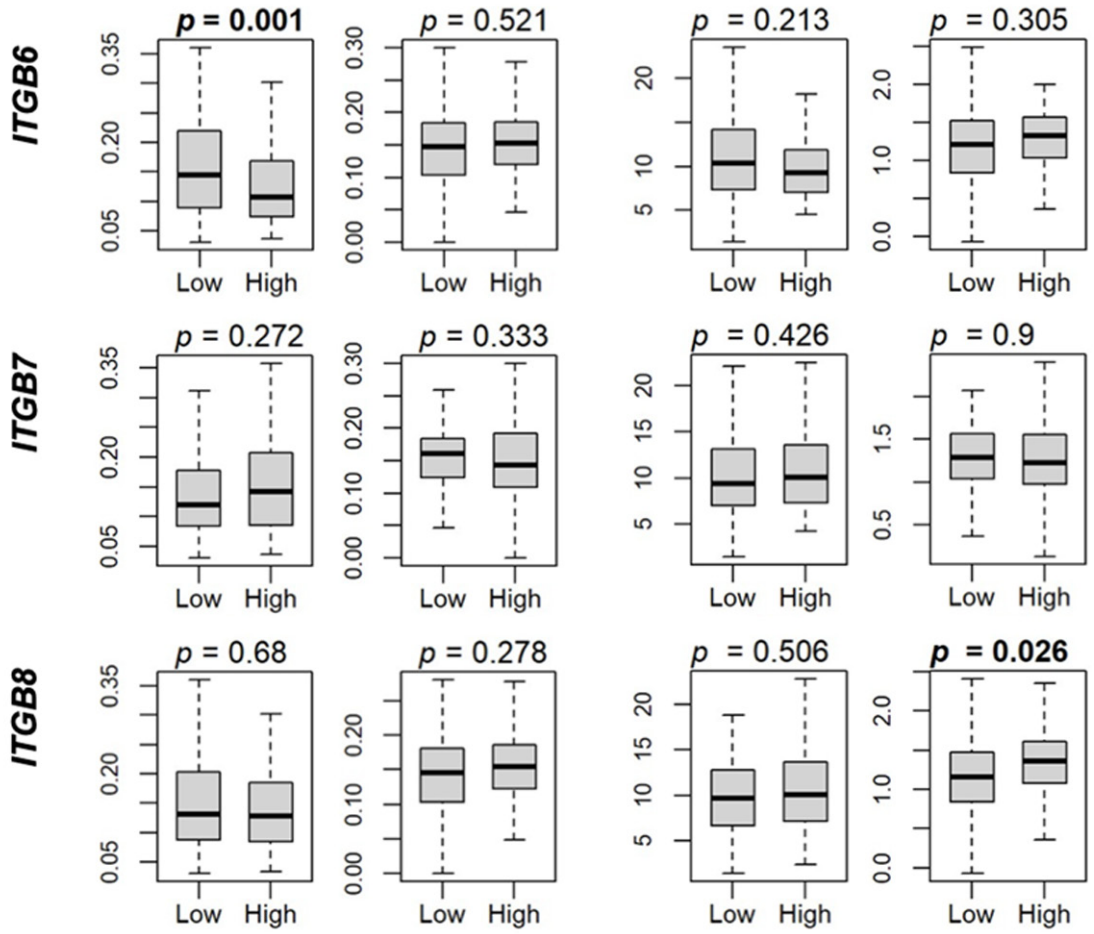

Figure 7. Endothelial cell composition correlation with beta integrin expression in PDACs. A. Box plots of endothelial cell composition based on the x-Cell algorithm for the TCGA and GSE21501 cohorts. B. Box plots of endothelial cell composition based on the MCP-counter algorithm for the TCGA and GSE21501 cohorts. The bolded center bar in each box plot represents the median, the lower and upper bounds of the box represent the 25th and 75th percentiles, respectively, and the lower and upper tails represent the minimum and maximum values, respectively. Beta-integrin expression is dichotomized into high and low groups by the median, with n=177 for the TCGA cohort and n=132 for the GSE21501 cohort.

unique in that it does not affect patient outcomes, whereas high expression of the other integrins all decreased PFS, DFS, DSS, and OS. Experimental murine models have shown that knockout of integrin β5 decreases tumor burden and prolonged survival, and peptide targeting of the αvβ5 integrin increases tumor drug delivery [41]. A survey of effects of short-hair pin RNA knockdown of *ITGAV* in pancreatic cancer cell culture decreases *ITGB1* expression by 31% and *ITGB6* by 73% [42]. Antibody targeting of integrin αvβ6 increases gemcitabine delivery to mice with subcutaneous pancreatic tumors, resulting in a significant survival benefit, and antibody monotherapy in these tumors significantly decreases collagen disposition [43]. Integrin αvβ6 overexpression is accompanied by a poorer overall survival for multiple cancer types besides pancreatic cancer, with the key mechanism believed to be integrin dependent activation of TGF-β1 and subsequent stimulation of the EMT process [43, 44]. There is no literature on the relationship between *ITGB2* expression and pancreatic cancer. It is possible that *ITGB2* could have signaling redundancy in the context of targeted therapy against *ITGB1, 5,* or *6*, and this postulation should be considered in further investigations.

We observed that high-*ITGB4* tumor expression is unique with significantly decreased tumor fibroblast composition and worse PFS and DFS.

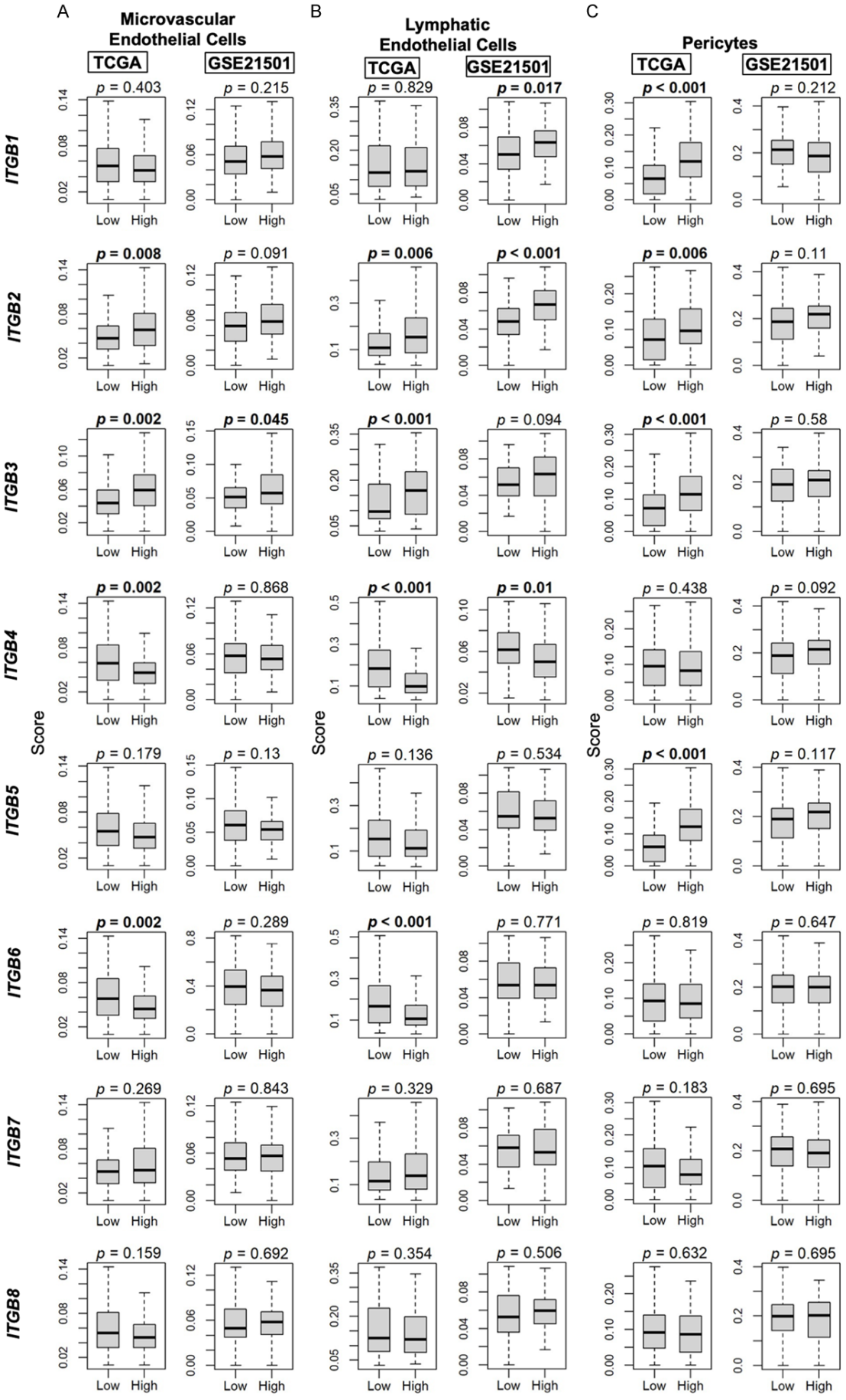
A
Microvascular Endothelial Cells
B
Lymphatic Endothelial Cells
C
Pericytes
TCGA
GSE21501
ITGB1
ITGB2
ITGB3
ITGB4
ITGB5
ITGB6
ITGB7
ITGB8
Score
Low
High
p = 0.403
p = 0.215
p = 0.829
p = 0.017
p < 0.001
p = 0.212
p = 0.008
p = 0.091
p = 0.006
p < 0.001
p = 0.006
p = 0.11
p = 0.002
p = 0.045
p < 0.001
p = 0.094
p < 0.001
p = 0.58
p = 0.002
p = 0.868
p < 0.001
p = 0.01
p = 0.438
p = 0.092
p = 0.179
p = 0.13
p = 0.136
p = 0.534
p < 0.001
p = 0.117
p = 0.002
p = 0.289
p < 0.001
p = 0.771
p = 0.819
p = 0.647
p = 0.269
p = 0.843
p = 0.329
p = 0.687
p = 0.183
p = 0.695
p = 0.159
p = 0.692
p = 0.354
p = 0.506
p = 0.632
p = 0.695

Figure 8. Microvascular endothelial cell, lymphatic endothelial cell, and pericyte composition correlation with beta integrin expression in PDACs. A. Box plots of the microvasular endothelial cell composition based on the x-Cell algorithm for the TCGA and GSE21501 cohorts. B. Box plots of lymphatic endothelial cell composition based on the xCell algorithm for the TCGA and GSE21501 cohorts. C. Box plots of pericyte composition based on the xCell algorithm for the TCGA and GSE21501 cohorts. The bolded center bar in each box plot represents the median, the lower and upper bounds of the box represent the 25th and 75th percentiles, respectively, and the lower and upper tails represent the minimum and maximum values, respectively. Beta-integrin expression is dichotomized into high and low groups by the median, with n=177 for the TCGA cohort and n=132 for the GSE21501 cohort.

Figure 9. Anti-cancerous immune cell correlation with beta integrin expression in PDACs. Box plots are based on the xCell algorithm for the TCGA and GSE21501 cohorts. The bolded center bar in each box plot represents the median, the lower and upper bounds of the box represent the 25th and 75th percentiles, respectively, and the lower and upper tails represent the minimum and maximum values, respectively. Beta-integrin expression is dichotomized into high

and low groups by the median, with n=177 for the TCGA cohort and n=132 for the GSE21501 cohort. Th1, T helper cell 1; M1, Macrophage type 1; DC, Dendritic Cell.

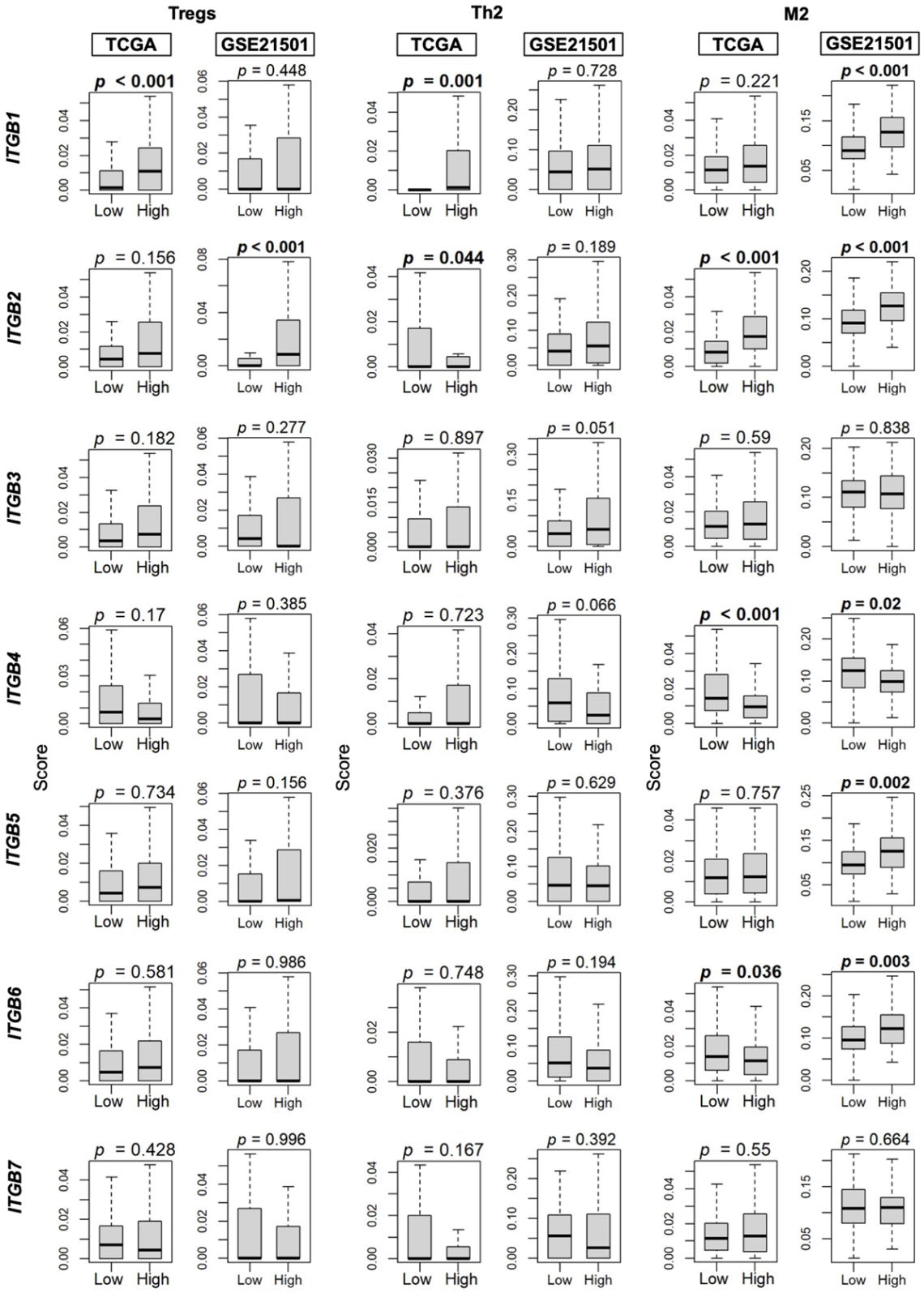

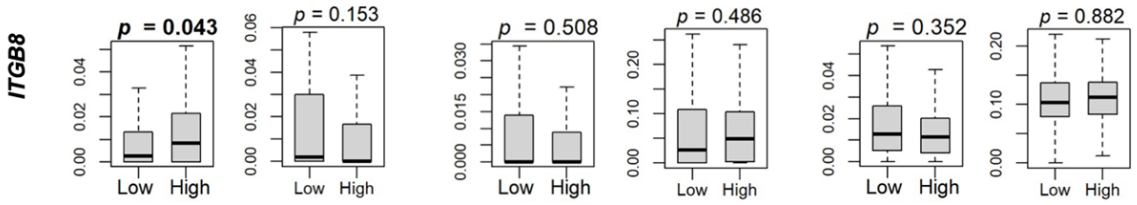

Figure 10. Pro-cancerous immune cell correlation with beta integrin expression in PDACs. Box plots are based on the xCell algorithm for the TCGA and GSE21501 cohorts. The bolded center bar in each box plot represents the median, the lower and upper bounds of the box represent the 25th and 75th percentiles, respectively, and the lower and upper tails represent the minimum and maximum values, respectively. Beta-integrin expression is dichotomized into high and low groups by the median, with n=177 for the TCGA cohort and n=132 for the GSE21501 cohort. Tregs, regulatory T cells; Th2, T helper cell 2; M2, Macrophage type 2.

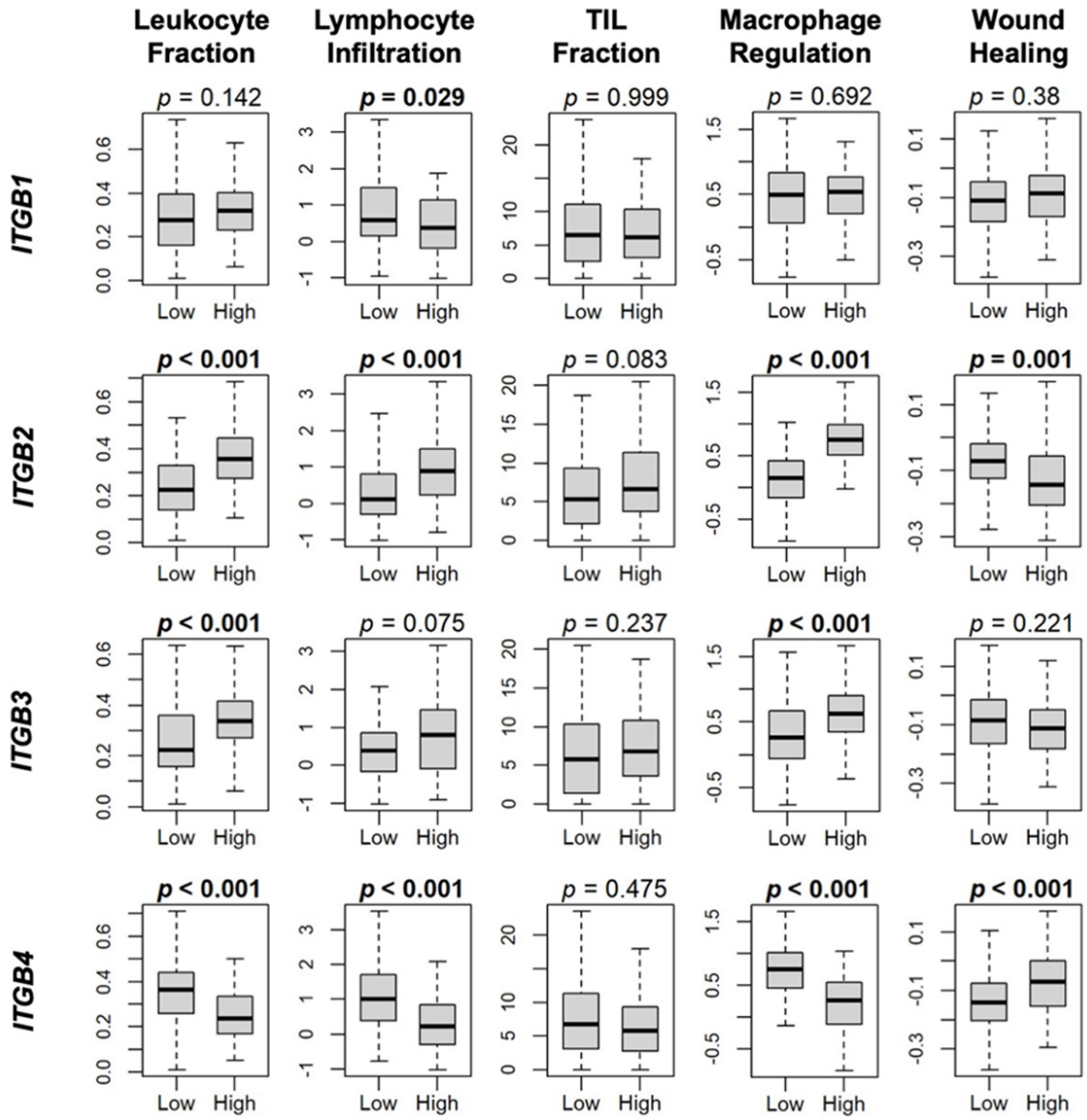

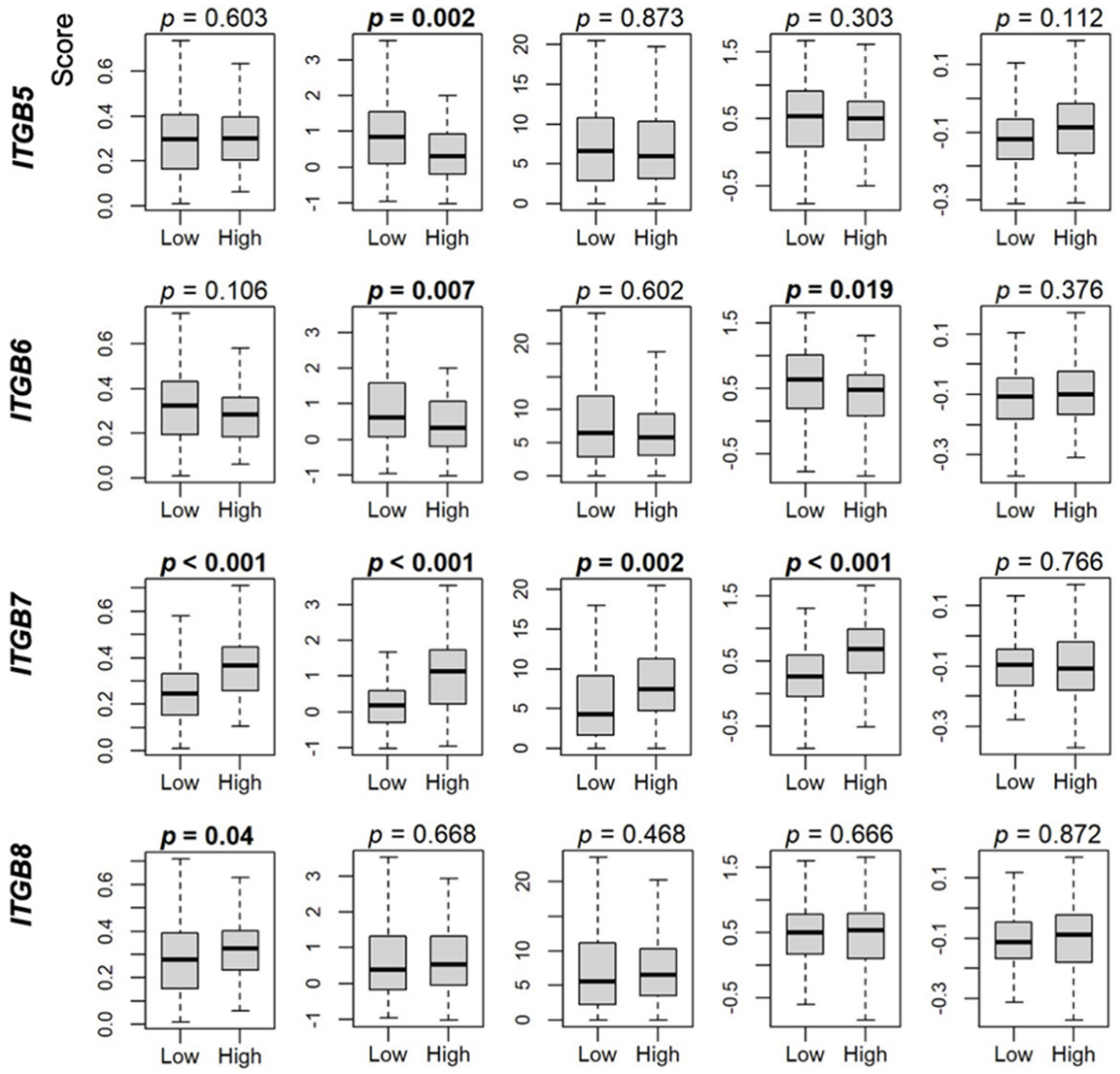

Figure 11. Immune scores for markers of tumor immune cell populations. Data is based on the scores by Throsson, *et al.* [37]. The bolded center bar in each box plot represents the median, the lower and upper bounds of the box represent the 25th and 75th percentiles, respectively, and the lower and upper tails represent the minimum and maximum values, respectively. Beta-integrin expression is dichotomized into high and low groups by the median, with n=177 for the TCGA cohort and n=132 for the GSE21501 cohort. TIL, Tumor Infiltration Lymphocyte.

High *ITGB4* expression is known to produce a highly metastatic phenotype through dimerization with integrin α6 and activation of MEK1-ERK1/2 signaling pathways [45]. Some studies have additionally theorized that a stroma-dense environment could slow metastasis essentially by restricting access to systemic lymphatic and hematogenous vasculature [40, 46]. In support of this idea, sonic-hedgehog-deficient PDACs have less stroma with resultant increased proliferation and metastatic phenotypes [46], and sonic hedgehog ligand expression results in a 4.5-fold decrease in *ITGB4* expression [47].

Overall, our results would suggest that the major effect of beta integrin signaling in PDACs is to create a fortress microenvironment that shields the tumor from the immune system. This is reflected in poor tumor infiltration of immune cells and essentially unchanged CYT scores apart from a statistically significant increase in high *ITGB2*-tumors in both the TCGA and GSE21501 cohorts. This most likely reflects the primarily understood role of β2 integrin biology to recognize sites of inflammation and recruit immune cells [48]. However, *ITGB2* expression does not correlate with differences in patient survival, again suggesting that pan-

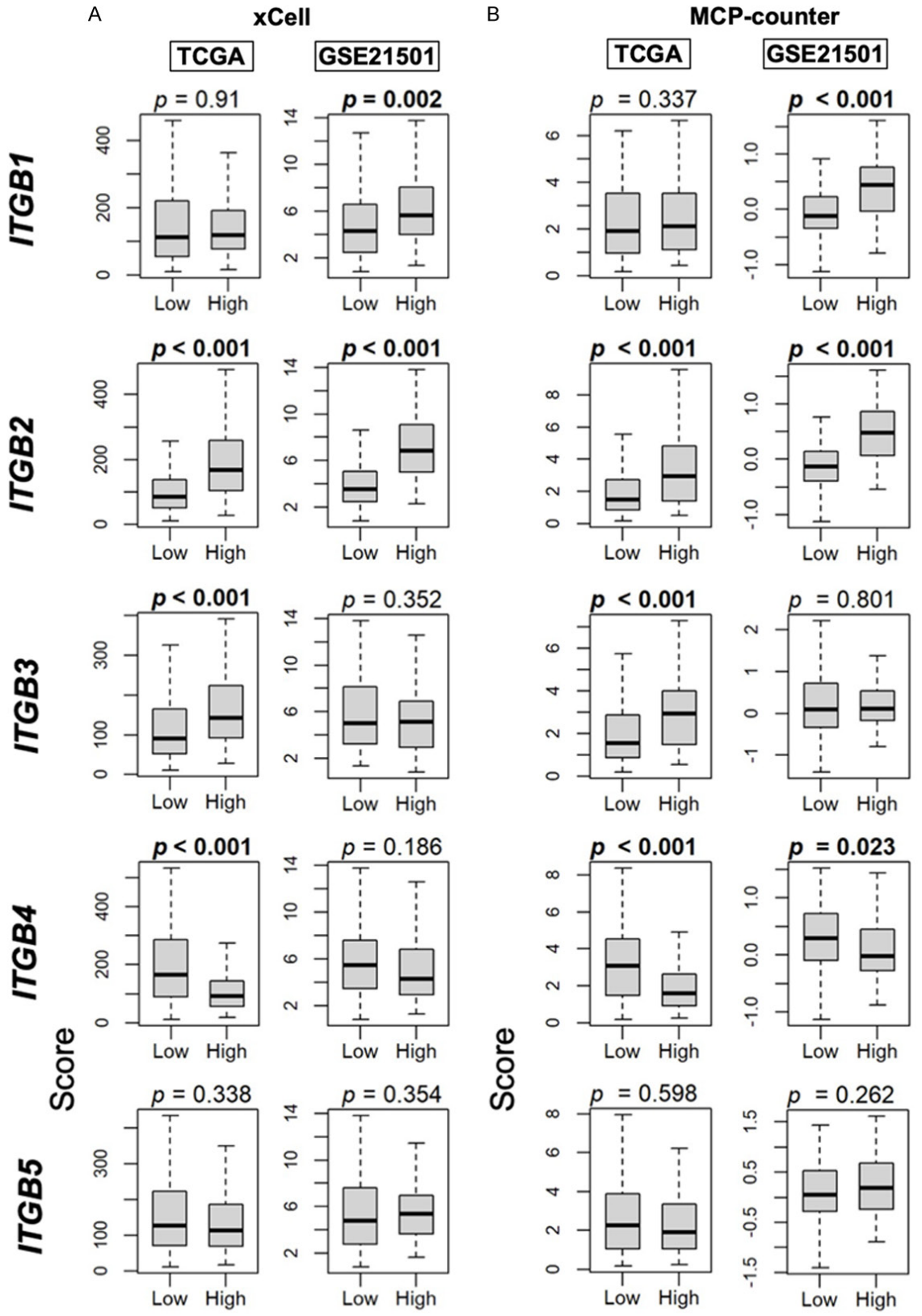
A
xCell
TCGA
GSE21501
B
MCP-counter
TCGA
GSE21501
ITGB1
ITGB2
ITGB3
ITGB4
ITGB5
Score
Score
p = 0.91
p = 0.002
p = 0.337
p < 0.001
p < 0.001
p < 0.001
p < 0.001
p < 0.001
p < 0.001
p = 0.352
p < 0.001
p = 0.801
p < 0.001
p = 0.186
p < 0.001
p = 0.023
p = 0.338
p = 0.354
p = 0.598
p = 0.262
Low
High

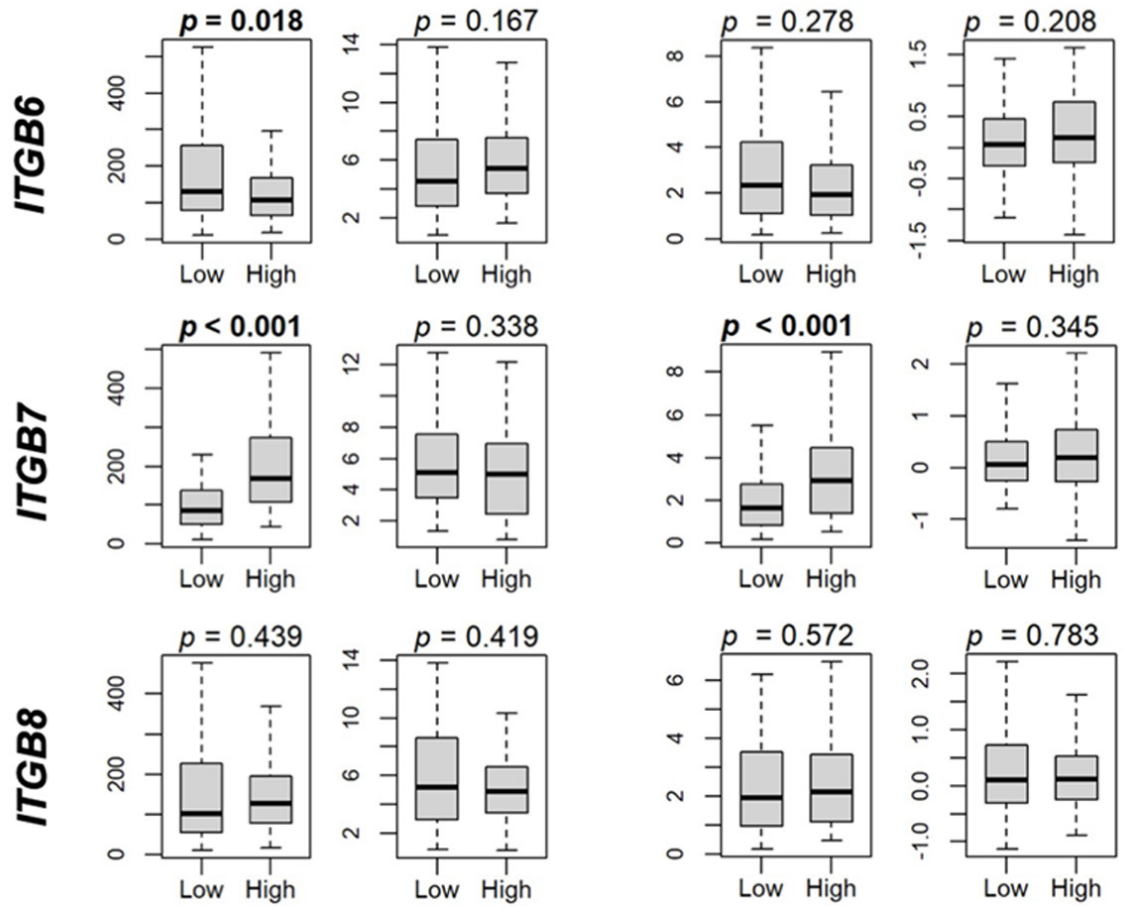

Figure 12. Cytolytic (CYT) score correlation with beta integrin expression in PDACs. A. Results from the xCell algorithm. B. Results from the MCP-counter algorithm. The bolded center bar in each box plot represents the median, the lower and upper bounds of the box represent the 25th and 75th percentiles, respectively, and the lower and upper tails represent the minimum and maximum values, respectively. Beta-integrin expression is dichotomized into high and low groups by the median, with n=177 for the TCGA cohort and n=132 for the GSE21501 cohort.

creatic tumor stroma blocks effective immune recognition of tumorigenesis.

As a retrospective analysis, our study does have several limitations. Although we have validated key findings with two independent cohorts, patient populations and treatments are heterogenous, which can easily affect outcomes. Bioinformatics data does not necessarily imply mechanisms of action, but it can provide powerful insights into the complex relationship of the TME that cannot be readily replicated in experimental models. Additionally, our findings that high *ITGB1*, *4, 5*, and *6* expression have redundant and complementary negative effects on patient outcomes is supported by another study that established a poor prognostic signature based on high expression levels of these four integrins in PDACs [49]. Our study found that increased tumor stroma density correlates to this poor prognostic signature.

In summary, the overarching conclusion from our study is that targeted beta integrin therapy has significant potential utility to improve PDAC treatment. However, such therapy must consider the significant redundancy demonstrated by multiple integrins exhibiting similar phenotypes. Further, because integrins exist as αβ heterodimers, their signaling effects can be further modulated by the nature of their pairings. Since redundancy in biology tends to imply evolutionary significance to function, we wish to encourage deeper research into targeting beta integrin signaling in tumor biology.

Acknowledgements

This research was supported by the National Institutes of Health, USA grant number R37CA248018, R01CA250412, R01CA251545, R01EB029596, the US Department of Defense BCRP grant numbers W81XWH-19-1-0674 and W81XWH-19-1-0111 to K.T., and the National Cancer Institute Cancer Center Support Grant P30CA016056 to Roswell Park Comprehensive Cancer Center.

Disclosure of conflict of interest

None.

Address correspondence to: Dr. Kazuaki Takabe, Department of Surgical Oncology, Roswell Park Comprehensive Cancer Center, Elm & Carlton Streets, Buffalo, New York 14263, USA. Tel: 716-845-5540; E-mail: kazuaki.takabe@roswellpark.org

References

[1] Siegel RL, Miller KD, Fuchs HE and Jemal A. Cancer statistics, 2022. CA Cancer J Clin 2022; 72: 7-33.

[2] Islami F, Ward EM, Sung H, Cronin KA, Tangka FKL, Sherman RL, Zhao J, Anderson RN, Henley SJ, Yabroff KR, Jemal A and Benard VB. Annual report to the nation on the status of cancer, part 1: national cancer statistics. J Natl Cancer Inst 2021; 113: 1648-1669.

[3] Kane S, Engelhart A, Guadagno J, Jones A, Usoro I and Brutcher E. Pancreatic ductal adenocarcinoma: characteristics of tumor microenvironment and barriers to treatment. J Adv Pract Oncol 2020; 11: 693-698.

[4] Wang S, Zheng Y, Yang F, Zhu L, Zhu XQ, Wang ZF, Wu XL, Zhou CH, Yan JY, Hu BY, Kong B, Fu DL, Bruns C, Zhao Y, Qin LX and Dong QZ. The molecular biology of pancreatic adenocarcinoma: translational challenges and clinical perspectives. Signal Transduct Target Ther 2021; 6: 249.

[5] Takada Y, Ye X and Simon S. The integrins. Genome Biol 2007; 8: 215.

[6] Mezu-Ndubuisi OJ and Maheshwari A. The role of integrins in inflammation and angiogenesis. Pediatr Res 2021; 89: 1619-1626.

[7] Hamidi H and Ivaska J. Every step of the way: integrins in cancer progression and metastasis. Nat Rev Cancer 2018; 18: 533-548.

[8] Li J, Peng L, Chen Q, Ye Z, Zhao T, Hou S, Gu J and Hang Q. Integrin β1 in pancreatic cancer: expressions, functions, and clinical implications. Cancers (Basel) 2022; 14: 3377.

[9] Seguin L, Kato S, Franovic A, Camargo MF, Lesperance J, Elliott KC, Yebra M, Mielgo A, Lowy AM, Husain H, Cascone T, Diao L, Wang J, Wistuba II, Heymach JV, Lippman SM, Desgrosellier JS, Anand S, Weis SM and Cheresh DA. An integrin β3-KRAS-RalB complex drives tumour stemness and resistance to EGFR inhibition. Nat Cell Biol 2014; 16: 457-468.

[10] Carbonell WS, DeLay M, Jahangiri A, Park CC and Aghi MK. β1 integrin targeting potentiates antiangiogenic therapy and inhibits the growth of bevacizumab-resistant glioblastoma. Cancer Res 2013; 73: 3145-3154.

[11] Schluterman MK, Chapman SL, Korpanty G, Ozumi K, Fukai T, Yanagisawa H and Brekken RA. Loss of fibulin-5 binding to β1 integrins inhibits tumor growth by increasing the level of ROS. Dis Model Mech 2010; 3: 333-342.

[12] Mia MS, Jarajapu Y, Rao R and Mathew S. Integrin β1 promotes pancreatic tumor growth by upregulating kindlin-2 and TGF-β receptor-2. Int J Mol Sci 2021; 22: 10599.

[13] Ferrara B, Pignatelli C, Cossutta M, Citro A, Courty J and Piemonti L. The extracellular matrix in pancreatic cancer: description of a complex network and promising therapeutic options. Cancers (Basel) 2021; 13: 4442.

[14] Brannon A 3rd, Drouillard D, Steele N, Schoettle S, Abel EV, Crawford HC and Pasca di Magliano M. Beta 1 integrin signaling mediates pancreatic ductal adenocarcinoma resistance to MEK inhibition. Sci Rep 2020; 10: 11133.

[15] Brown NF and Marshall JF. Integrin-mediated TGFβ activation modulates the tumour microenvironment. Cancers (Basel) 2019; 11: 1221.

[16] Sawai H, Okada Y, Funahashi H, Matsuo Y, Takahashi H, Takeyama H and Manabe T. Activation of focal adhesion kinase enhances the adhesion and invasion of pancreatic cancer cells via extracellular signal-regulated kinase-1/2 signaling pathway activation. Mol Cancer 2005; 4: 37.

[17] Su CY, Li JQ, Zhang LL, Wang H, Wang FH, Tao YW, Wang YQ, Guo QR, Li JJ, Liu Y, Yan YY and Zhang JY. The biological functions and clinical applications of integrins in cancers. Front Pharmacol 2020; 11: 579068.

[18] Almokadem S and Belani CP. Volociximab in cancer. Expert Opin Biol Ther 2012; 12: 251-257.

[19] Bell-McGuinn KM, Matthews CM, Ho SN, Barve M, Gilbert L, Penson RT, Lengyel E, Palaparthy R, Gilder K, Vassos A, McAuliffe W, Weymer S, Barton J and Schilder RJ. A phase II, single-arm study of the anti-α5β1 integrin antibody volociximab as monotherapy in patients with platinum-resistant advanced epithelial ovarian or

primary peritoneal cancer. Gynecol Oncol 2011; 121: 273-279.
[20] Besse B, Tsao LC, Chao DT, Fang Y, Soria JC, Almokadem S and Belani CP. Phase Ib safety and pharmacokinetic study of volociximab, an anti-α5β1 integrin antibody, in combination with carboplatin and paclitaxel in advanced non-small-cell lung cancer. Ann Oncol 2013; 24: 90-96.
[21] Benesch MG, Ko YM, McMullen TP and Brindley DN. Autotaxin in the crosshairs: taking aim at cancer and other inflammatory conditions. FEBS Lett 2014; 588: 2712-2727.
[22] Katsuta E, Huyser M, Yan L and Takabe K. A prognostic score based on long-term survivor unique transcriptomic signatures predicts patient survival in pancreatic ductal adenocarcinoma. Am J Cancer Res 2021; 11: 4294-4307.
[23] Tokumaru Y, Oshi M, Katsuta E, Yan L, Satyananda V, Matsuhashi N, Futamura M, Akao Y, Yoshida K and Takabe K. KRAS signaling enriched triple negative breast cancer is associated with favorable tumor immune microenvironment and better survival. Am J Cancer Res 2020; 10: 897-907.
[24] Oshi M, Patel A, Le L, Tokumaru Y, Yan L, Matsuyama R, Endo I and Takabe K. G2M checkpoint pathway alone is associated with drug response and survival among cell proliferation-related pathways in pancreatic cancer. Am J Cancer Res 2021; 11: 3070-3084.
[25] Oshi M, Tokumaru Y, Mukhopadhyay S, Yan L, Matsuyama R, Endo I and Takabe K. Annexin A1 expression is associated with epithelial-mesenchymal transition (EMT), cell proliferation, prognosis, and drug response in pancreatic cancer. Cells 2021; 10: 653.
[26] Takahashi H, Katsuta E, Yan L, Tokumaru Y, Katz MHG and Takabe K. Transcriptomic profile of lymphovascular invasion, a known risk factor of pancreatic ductal adenocarcinoma metastasis. Cancers (Basel) 2020; 12: 2033.
[27] Katsuta E, Qi Q, Peng X, Hochwald SN, Yan L and Takabe K. Pancreatic adenocarcinomas with mature blood vessels have better overall survival. Sci Rep 2019; 9: 1310.
[28] Lonsdale J, Thomas J, Salvatore M, Phillips R, Lo E, Shad S, Hasz R, Walters G, Garcia F, Young N, Foster B, Moser M, Karasik E, Gillard B, Ramsey K, Sullivan S, Bridge J, Magazine H, Syron J, Fleming J, Siminoff L, Traino H, Mosavel M, Barker L, Jewell S, Rohrer D, Maxim D, Filkins D, Harbach P, Cortadillo E, Berghuis B, Turner L, Hudson E, Feenstra K, Sobin L, Robb J, Branton P, Korzeniewski G, Shive C, Tabor D, Qi L, Groch K, Nampally S, Buia S, Zimmerman A, Smith A, Burges R, Robinson K, Valentino K, Bradbury D, Cosentino M, Diaz-Mayoral N, Kennedy M, Engel T, Williams P, Erickson K, Ardlie K, Winckler W, Getz G, DeLuca D, MacArthur D, Kellis M, Thomson A, Young T, Gelfand E, Donovan M, Meng Y, Grant G, Mash D, Marcus Y, Basile M, Liu J, Zhu J, Tu Z, Cox NJ, Nicolae DL, Gamazon ER, Im HK, Konkashbaev A, Pritchard J, Stevens M, Flutre T, Wen X, Dermitzakis ET, Lappalainen T, Guigo R, Monlong J, Sammeth M, Koller D, Battle A, Mostafavi S, McCarthy M, Rivas M, Maller J, Rusyn I, Nobel A, Wright F, Shabalin A, Feolo M, Sharopova N, Sturcke A, Paschal J, Anderson JM, Wilder EL, Derr LK, Green ED, Struewing JP, Temple G, Volpi S, Boyer JT, Thomson EJ, Guyer MS, Ng C, Abdallah A, Colantuoni D, Insel TR, Koester SE, Little AR, Bender PK, Lehner T, Yao Y, Compton CC, Vaught JB, Sawyer S, Lockhart NC, Demchok J and Moore HF. The genotype-tissue expression (GTEx) project. Nat Genet 2013; 45: 580-585.
[29] Subramanian A, Tamayo P, Mootha VK, Mukherjee S, Ebert BL, Gillette MA, Paulovich A, Pomeroy SL, Golub TR, Lander ES and Mesirov JP. Gene set enrichment analysis: a knowledge-based approach for interpreting genome-wide expression profiles. Proc Natl Acad Sci U S A 2005; 102: 15545-15550.
[30] Liberzon A, Birger C, Thorvaldsdóttir H, Ghandi M, Mesirov JP and Tamayo P. The molecular signatures database (MSigDB) hallmark gene set collection. Cell Syst 2015; 1: 417-425.
[31] Aran D, Hu Z and Butte AJ. xCell: digitally portraying the tissue cellular heterogeneity landscape. Genome Biol 2017; 18: 220.
[32] Tokumaru Y, Oshi M, Murthy V, Tian W, Yan L, Angarita FA, Nagahashi M, Matsuhashi N, Futamura M, Yoshida K, Miyoshi Y and Takabe K. Low intratumoral genetic neutrophil-to-lymphocyte ratio (NLR) is associated with favorable tumor immune microenvironment and with survival in triple negative breast cancer (TNBC). Am J Cancer Res 2021; 11: 5743-5755.
[33] Chouliaras K, Oshi M, Asaoka M, Tokumaru Y, Khoury T, Endo I, Ishikawa T and Takabe K. Increased intratumor heterogeneity, angiogenesis and epithelial to mesenchymal transition pathways in metaplastic breast cancer. Am J Cancer Res 2021; 11: 4408-4420.
[34] Le L, Tokumaru Y, Oshi M, Asaoka M, Yan L, Endo I, Ishikawa T, Futamura M, Yoshida K and Takabe K. Th2 cell infiltrations predict neoadjuvant chemotherapy response of estrogen receptor-positive breast cancer. Gland Surg 2021; 10: 154-165.
[35] Oshi M, Asaoka M, Tokumaru Y, Angarita FA, Yan L, Matsuyama R, Zsiros E, Ishikawa T, Endo I and Takabe K. Abundance of regulatory T cell (Treg) as a predictive biomarker for neoadjuvant chemotherapy in triple-negative

breast cancer. Cancers (Basel) 2020; 12: 3038.
[36] Becht E, Giraldo NA, Lacroix L, Buttard B, Elarouci N, Petitprez F, Selves J, Laurent-Puig P, Sautès-Fridman C, Fridman WH and de Reyniès A. Estimating the population abundance of tissue-infiltrating immune and stromal cell populations using gene expression. Genome Biol 2016; 17: 218.
[37] Thorsson V, Gibbs DL, Brown SD, Wolf D, Bortone DS, Ou Yang TH, Porta-Pardo E, Gao GF, Plaisier CL, Eddy JA, Ziv E, Culhane AC, Paull EO, Sivakumar IKA, Gentles AJ, Malhotra R, Farshidfar F, Colaprico A, Parker JS, Mose LE, Vo NS, Liu J, Liu Y, Rader J, Dhankani V, Reynolds SM, Bowlby R, Califano A, Cherniack AD, Anastassiou D, Bedognetti D, Mokrab Y, Newman AM, Rao A, Chen K, Krasnitz A, Hu H, Malta TM, Noushmehr H, Pedamallu CS, Bullman S, Ojesina AI, Lamb A, Zhou W, Shen H, Choueiri TK, Weinstein JN, Guinney J, Saltz J, Holt RA, Rabkin CS, Lazar AJ, Serody JS, Demicco EG, Disis ML, Vincent BG and Shmulevich I. The immune landscape of cancer. Immunity 2018; 48: 812-830, e814.
[38] Wakiyama H, Masuda T, Motomura Y, Hu Q, Tobo T, Eguchi H, Sakamoto K, Hirakawa M, Honda H and Mimori K. Cytolytic activity (CYT) score is a prognostic biomarker reflecting host immune status in hepatocellular carcinoma (HCC). Anticancer Res 2018; 38: 6631-6638.
[39] Fusco MJ, West H and Walko CM. Tumor mutation burden and cancer treatment. JAMA Oncol 2021; 7: 316.
[40] Provenzano PP and Hingorani SR. Hyaluronan, fluid pressure, and stromal resistance in pancreas cancer. Br J Cancer 2013; 108: 1-8.
[41] Hurtado de Mendoza T, Mose ES, Botta GP, Braun GB, Kotamraju VR, French RP, Suzuki K, Miyamura N, Teesalu T, Ruoslahti E, Lowy AM and Sugahara KN. Tumor-penetrating therapy for β5 integrin-rich pancreas cancer. Nat Commun 2021; 12: 1541.
[42] Kemper M, Schiecke A, Maar H, Nikulin S, Poloznikov A, Galatenko V, Tachezy M, Gebauer F, Lange T, Riecken K, Tonevitsky A, Aigner A, Izbicki J, Schumacher U and Wicklein D. Integrin alpha-V is an important driver in pancreatic adenocarcinoma progression. J Exp Clin Cancer Res 2021; 40: 214.
[43] Reader CS, Vallath S, Steele CW, Haider S, Brentnall A, Desai A, Moore KM, Jamieson NB, Chang D, Bailey P, Scarpa A, Lawlor R, Chelala C, Keyse SM, Biankin A, Morton JP, Evans TJ, Barry ST, Sansom OJ, Kocher HM and Marshall JF. The integrin αvβ6 drives pancreatic cancer through diverse mechanisms and represents an effective target for therapy. J Pathol 2019; 249: 332-342.
[44] Bates RC, Bellovin DI, Brown C, Maynard E, Wu B, Kawakatsu H, Sheppard D, Oettgen P and Mercurio AM. Transcriptional activation of integrin β6 during the epithelial-mesenchymal transition defines a novel prognostic indicator of aggressive colon carcinoma. J Clin Invest 2005; 115: 339-347.
[45] Meng X, Liu P, Wu Y, Liu X, Huang Y, Yu B, Han J, Jin H and Tan X. Integrin beta 4 (ITGB4) and its tyrosine-1510 phosphorylation promote pancreatic tumorigenesis and regulate the MEK1-ERK1/2 signaling pathway. Bosn J Basic Med Sci 2020; 20: 106-116.
[46] Rhim AD, Oberstein PE, Thomas DH, Mirek ET, Palermo CF, Sastra SA, Dekleva EN, Saunders T, Becerra CP, Tattersall IW, Westphalen CB, Kitajewski J, Fernandez-Barrena MG, Fernandez-Zapico ME, Iacobuzio-Donahue C, Olive KP and Stanger BZ. Stromal elements act to restrain, rather than support, pancreatic ductal adenocarcinoma. Cancer Cell 2014; 25: 735-747.
[47] Damhofer H, Medema JP, Veenstra VL, Badea L, Popescu I, Roelink H and Bijlsma MF. Assessment of the stromal contribution to Sonic Hedgehog-dependent pancreatic adenocarcinoma. Mol Oncol 2013; 7: 1031-1042.
[48] Harjunpää H, Llort Asens M, Guenther C and Fagerholm SC. Cell adhesion molecules and their roles and regulation in the immune and tumor microenvironment. Front Immunol 2019; 10: 1078.
[49] Zhuang H, Zhou Z, Ma Z, Li Z, Liu C, Huang S, Zhang C and Hou B. Characterization of the prognostic and oncologic values of ITGB superfamily members in pancreatic cancer. J Cell Mol Med 2020; 24: 13481-13493.